where

$$C_k' = C_k + \eta;$$

(A8b)

and that of the average $\Lambda$-nucleon potential (2.1b) divided by $-U_0$ is

$$P = \sum_{i,j,k=1}^{3} d_{ijk} K(A_i', B_j, C_k),$$

(A9a)

where

$$A_i' = A_i + \lambda.$$

(A9b)

The parameters $\eta$ and $\lambda$ are the potential range parameters given in (2.1).

---

# Propagation of the Single-Scattering Distribution in Multiple Scattering: Muon Scattering in Iron*

NORRIS A. NICKOLS† AND WALTER H. BARKAS
*Lawrence Radiation Laboratory, University of California, Berkeley, California*
(Received 26 October 1962)

The moments of the projected angular distribution of the single-scattering process are shown to be derivable from the emergent angular distribution of a beam that has traversed a thick absorber. Since very small deflections do not contribute to the observed moments, ambiguity is avoided by adopting a formulation of the electronic screening that leads to a definite total scattering cross section. The theory is applied to an experiment in which 2-BeV muons are incident on an iron scatterer 18 in. thick. The observed angular distribution is analyzed. It is shown that the nuclear electromagnetic form factor derived from the muon data is consistent with that found from electron scattering, and is completely incompatible with a point-nucleus model.

## I. INTRODUCTION

BECAUSE they are thought to interact only with the distribution of charges and currents in an atomic nucleus, charged leptons have been considered excellent probes for a study of the detailed structure of atomic nuclei. Extensive use has already been made of electrons for this purpose.[1] In some respects muons should be even better suited for this task, but until recently the only "beams" of muons available were those of the cosmic rays. A complication also was introduced when muons were reported to scatter[2,3] as predicted by the Molière theory,[4] which is inapplicable if the nucleus cannot be represented by a point charge.

In this paper we describe an experiment designed to study this question. Since it was initiated, however, results have been reported by other investigators that leave little reason to believe that the muon scatters anomalously. Decisive experiments were carried out by Connelly et al.,[5] Masek et al.,[6] Kim et al.,[7] Citron et al.,[8] and others. Our results, therefore, are merely confirmatory, but in obtaining them we have introduced a new method for analyzing the data that presumably has utility for many related problems in high-energy physics.

After a beam of particles has penetrated a finite

---

[1] R. Hofstadter, Ann. Rev. Nucl. Sci. 7, 237–316 (1957).
[2] J. L. Lloyd and A. W. Wolfendale, Proc. Phys. Soc. (London) A68, 1045 (1955).
[3] I. B. McDiarmid, Phil. Mag. 46, 177 (1955); W. L. Whittemore and R. P. Shutt, Phys. Rev. 88, 1312 (1952); and J. L. Lloyd, E. Rossle, and A. W. Wolfendale, Proc. Phys. Soc. (London) A70, 421 (1957). [Summary of muon experiments to 1958 in: G. N. Fowler and A. W. Wolfendale, *Progress in Elementary Particle and Cosmic-Ray Physics*, edited by J. G. Wilson and S. A. Wouthuysen (North-Holland Publishing Company, Amsterdam, Holland, 1958), Vol. 4, p. 123.]

[4] G. Molière, Z. Naturforsch 2a, 133 (1947); 32, 78 (1948); H. A. Bethe, Phys. Rev. 89, 1256 (1953).
[5] P. L. Connolly, J. G. McEwan, and J. Orear, Phys. Rev. Letters 6, 554 (1961).
[6] G. E. Masek, L. D. Heggie, Y. K. Kim, and R. W. Williams, Phys. Rev. 122, 937 (1961).
[7] C. Y. Kim, S. Kaneko, Y. B. Kim, G. E. Masek, and R. W. Williams, Phys. Rev. 122, 1641 (1961).
[8] A. Citron, C. Delorme, D. Fries, L. Goldzahl, J. Heintze, E. G. Michaelis, C. Richard, and H. Øverås, Phys. Letters 1, 175 (1962).

thickness of matter, its angular distribution inevitably is contaminated by a component of plural or multiple-scattering events. The magnitude of the effect increases with the absorber thickness. To study the rare large single deflections of high-energy muons, however, it is most practical to use a relatively thick absorber because it will tend to keep the required intensity and/or time of exposure moderate. But then the primary scattering distribution may be largely obscured by the plural and multiple small-angle scattering.

The multiple-scattering distribution can be calculated from a known elementary (single) scattering distribution if one uses the method introduced by Snyder and Scott.[9] It is limited to small angles, however.

Suppose that in an elementary-scattering event the probability that the particle be deflected between a projected angle $\omega$ and $\omega + d\omega$ is $\rho(\omega)d\omega$. (Whether an angular distribution is projected or not is immaterial; to transform a projected distribution to the corresponding spatial distribution, one inverts an integral equation of a standard Abel type.) We shall assume that $\rho$ is an even function of $\omega$—the discussion of the scattering of polarized beams would require odd terms in addition. Let the total scattering cross section be $\sigma$, so that in a path $t$ the average number of times the particle experiences a deflection between $\omega$ and $\omega + d\omega$ is $N\sigma t\rho(\omega)d\omega$, the number of atoms per unit volume being $N$. Then, after the particle has penetrated the scattering material a distance $t$, the probability that it will have been deflected in the projected angular interval $\phi$ to $\phi + d\phi$ is $f(\phi,t)d\phi$. By use of the method of Snyder and Scott, we can calculate $f(\phi,t)$ from

$$f(\phi,t) = \frac{\exp(-N\sigma t)}{\pi} \int_{S=-\infty}^{\infty} \cos(\phi S)$$

$$\times \exp\left[N\sigma t \int_{-\infty}^{\infty} \rho(\omega) \cos(S\omega)d\omega\right] dS. \quad (1)$$

The inverse process of obtaining the elementary-scattering distribution from the observed distribution of multiple-scattering angles has been much more difficult to carry out in a practical way. Therefore, to relate the observed multiple-scattering distribution to the elementary-scattering distribution, we studied the propagation of the moments of the elementary-scattering distribution through many elementary acts of scattering. We found a set of simple and important connections existing between the moments of the single- and multiple-scattering distributions. These are of wide general applicability, as will be seen in Sec. II.

To investigate the scattering of muons in carbon, lead, and emulsion, Masek et al.[6] and Kim et al.[7] recently developed a beam of 2.0-BeV muons. Such muons have a shorter wavelength than any other machine-accelerated leptons previously used for nuclear probes,

and, in principle, can yield more detailed information about nuclear structure, if the basic assumptions regarding the nuclear scattering of muons are correct.

The existence of the Masek beam led us to examine its multiple scattering in iron. We have found on analyzing this distribution that the method of propagated moments is practical. In particular, when we apply the appropriate equations to our data, they disclose that the scattering from the iron nucleus differs greatly from the Molière distribution. We find agreement with the scattering expected from an extended nucleus having a form factor approximately as deduced from electron scattering.

## II. RELATIONS BETWEEN THE MOMENTS OF THE SCATTERING DISTRIBUTIONS

Suppose $\omega_i$ is a typical independent projected angle of deflection in the elementary-scattering process. Then, after $n$ deflections, the resultant angle of deflection $\phi_n$ is the algebraic sum of the $\omega_i$:

$$\phi_n \equiv \phi = \sum_{i=1}^{n} \omega_i. \quad (2)$$

The expectation value of the $r$th moment of $\phi$ accordingly is

$$\langle \phi^r \rangle = \langle (\sum_{i=1}^{n} \omega_i)^r \rangle. \quad (3)$$

Now the $2m$th moment of the elementary-scattering distribution is the expectation value $\langle \omega_i^{2m} \rangle$ of the $2m$th power of a typical elementary-scattering deflection. All the moments of the multiple-scattering distribution, therefore, can be derived from the elementary-scattering distributions. Thus,

$$\langle \phi^2 \rangle = n\langle \omega^2 \rangle,$$

$$\langle \phi^4 \rangle = n\langle \omega^4 \rangle + 3n^2\langle \omega^2 \rangle^2,$$

$$\langle \phi^6 \rangle = n\langle \omega^6 \rangle + 15n^2\langle \omega^2 \rangle\langle \omega^4 \rangle + 15n^3\langle \omega^2 \rangle^3, \quad (4)$$

$$\langle \phi^8 \rangle = n\langle \omega^8 \rangle + 28n^2\langle \omega^6 \rangle\langle \omega^2 \rangle + 35n^2\langle \omega^4 \rangle^2$$

$$+ 210n^3\langle \omega^4 \rangle\langle \omega^2 \rangle^2 + 105n^4\langle \omega^2 \rangle^4,$$

etc., for $n \gg 1$.

For unpolarized particles odd moments do not occur and, in general,

$$d\langle \phi^{2m} \rangle/dn$$

$$= \sum_{j=1}^{m} (2m)! \langle \omega^{2j} \rangle\langle \phi^{2(m-j)} \rangle/[2(m-j)]!(2j)!. \quad (5)$$

The above equations can be easily inverted so that from the moments of the multiple-scattering distribution, we obtain the moments of the elementary distribution:

$$\langle \omega^2 \rangle = \langle \phi^2 \rangle/n,$$

$$\langle \omega^4 \rangle = (1/n)[\langle \phi^4 \rangle - 3\langle \phi^2 \rangle^2],$$

$$\langle \omega^6 \rangle = (1/n)[\langle \phi^6 \rangle - 15\langle \phi^4 \rangle\langle \phi^2 \rangle + 30\langle \phi^2 \rangle^3], \quad (6)$$

$$\langle \omega^8 \rangle = (1/n)[\langle \phi^8 \rangle - 28\langle \phi^6 \rangle\langle \phi^2 \rangle - 35\langle \phi^4 \rangle^2$$

$$+ 420\langle \phi^4 \rangle\langle \phi^2 \rangle^2 - 630\langle \phi^2 \rangle^4], \quad \text{etc.}$$

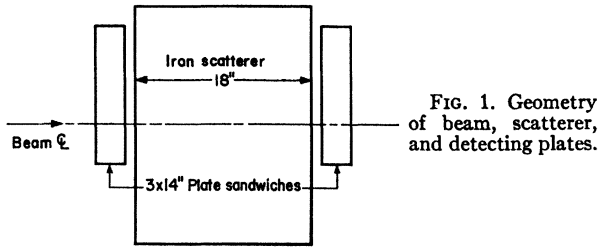[9] H. S. Snyder and W. T. Scott, Phys. Rev. 76, 220 (1949).

FIG. 1. Geometry of beam, scatterer, and detecting plates.

When $n$ is the average number of deflections $N\sigma t$ in path $t$, it is directly related to the total-scattering cross section. This cross section is undefined, however, unless a definite prescription for cutting off the very small deflections is adopted. These deflections do not contribute to the moments of the multiple-scattering distribution, and the $\langle\phi^{2m}\rangle$ are insensitive to the method adopted for treating the small deflections. The details of the electronic screening of the nucleus are uncritical except that $\rho(\omega)$ must be normalized so that the total cross section $\sigma$ is given by $\sigma=n/Nt$. As an example, Scott[10] gives an effective number of collisions

$$n=\frac{1.47\times10^{-20}Ntz^2Z^{1/3}(Z+1)}{\beta^2+(zZ/75)^2} \qquad (7)$$

in path $t$. Therefore, the total cross section with this screening is

$$\sigma=\frac{1.47\times10^{-20}z^2Z^{1/3}(Z+1)}{\beta^2+(zZ/75)^2}\text{ cm}^2,$$

regardless of the character of the nuclear scattering.

In the expression for the total scattering cross section, $ze$ is the charge carried by the moving particle, $Z$ is the atomic number of the scattering element, and $\beta c$ is the velocity of the moving particle. In the Molière formula we have followed the procedure of Bethe and Ashkin in putting $Z(Z+1)$ for $Z^2$ to allow something for incoherent scattering by electrons.[11]

A Gaussian in $\phi$ satisfies the condition

$$\langle\phi^4\rangle/\langle\phi^2\rangle^2=3, \qquad (8)$$

and for any elementary distribution

$$[\langle\phi^4\rangle/\langle\phi^2\rangle^2-3]\langle\phi^2\rangle$$

is a positive constant that is independent of $n$. Since $\langle\phi^2\rangle$ increases with $n$, the factor

$$[\langle\phi^4\rangle/\langle\phi^2\rangle^2-3]$$

must decrease. In accord with the central limit theorem,[12] it tends to satisfy the Gaussian condition.

[10] W. T. Scott, Phys. Rev. 85, 245 (1952).
[11] Hans A. Bethe and Julius Ashkin, in *Experimental Nuclear Physics*, edited by E. Segrè (John Wiley & Sons, Inc., New York, 1960), Vol. 1, p. 252.
[12] H. Cramèr, *Mathematical Methods of Statistics* (Princeton University Press, Princeton, New Jersey, 1946).

A distribution for which $\langle\phi^4\rangle/\langle\phi^2\rangle^2$ is greater than 3 is called *leptokurtic*.[13] All multiple-scattering distributions have the characteristic, and tend toward Gaussians for large $n$. For a finite absorber thickness, however, each even moment of the multiple-scattering distribution retains information regarding the elementary-scattering distribution. The higher moments are more sensitive to the kurtosis of the distribution than are the lower moments.

Thus far, it has been assumed that the moments of $\rho(\omega)$ do not depend on $n$. When the particle energy-loss rate is significant, however, $\rho(\omega)$ depends explicitly on $t$. Then we must write

$$d\langle\phi^{2m}\rangle/dt=N\sigma(t)$$
$$\times\sum_{j=1}^{m}(2m)!\langle\phi^{2(m-j)}\rangle\langle\omega^{2j}\rangle/[2(m-j)]!(2j)!. \qquad (9)$$

The magnitudes $\langle\phi^{2m}\rangle$ can be found by integrating these equations, given the dependence of $\rho(\omega)$ on $t$. It is not then possible, however, to reconstruct the moments of $\rho(\omega)$ at all $t$ from the observed moments of $f(\phi,t)$ at a single $t$.

## III. EXPERIMENTAL

### A. Beam and Scatterer

The projected angular distribution in the vertical plane of the beam of monoenergetic muons was measured before and after penetration of 18 in. of iron. The experimental arrangement is shown in Fig. 1. Muons, of median momentum 2.0±0.03 BeV/c, are incident upon the iron absorber which is behind the targets used by Masek *et al.* in their counter experiment. Emulsion stacks were placed ahead of and behind the first 18-in. portion of the absorber to determine the projected angular distributions of the beams at those points. Since an accidental burst of pions in the beam would have contaminated the emulsion enough to ruin the experiment, two separate runs were made, each in complete compatibility with the counter experiment. Each run lasted about 3 days, during which the counter experiment was done with carbon targets, with lead targets, and with no target. No accidental pion contamination was detected in either run by the counters or the emulsions. All the data in this study are from the first run.

### B. Plate Sandwiches

To eliminate the background of old cosmic-ray tracks from our experiment, pairs of large $3\times14$-in.$\times600\mu$
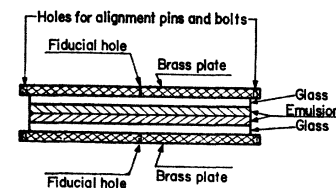


FIG. 2. Assembly of detecting plates. The beam was generally parallel to the plane of the emulsion.

[13] P. G. Hoel, *Introduction to Mathematical Statistics* (John Wiley & Sons, Inc., New York, 1954).
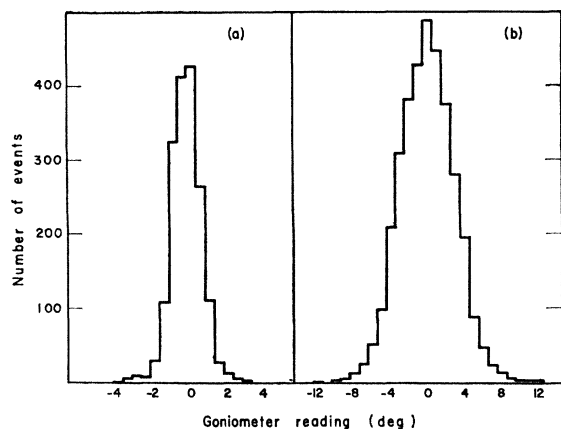
FIG. 3. Projected angular distribution of the beam:
(a) incident, and (b) emergent.

Ilford K.5 emulsion plates were clamped face to face during the exposure. After processing, the pair of plates could be accurately reassembled in their original relative position. Then, only the tracks that continue in the second layer of emulsion after crossing the interface were part of the beam in this experiment. A cross section of the emulsion sandwich is shown in Fig. 2. Holes around the edge for the tight-fitting alignment pins and small holes in the center for fiducial marks were drilled in each pair of brass plates while they were clamped together. The sandwiches were bolted together in the darkroom with the alignment pins in place. With the edges taped light tight, each fiducial hole was exposed to the light from a small flashlight for a few seconds and then taped. The exposures produced small fiducial marks on the glass side of each emulsion layer. These marks facilitated their subsequent realignment.

After processing, emulsion pairs were bolted together in the same orientation with small steel frames glued to the ends of each glass mounting plate—a layer of immersion oil provided optical contact between the emulsions and we made final adjustments by aligning the prongs of stars traced through the interface, using thumbscrews affixed to the steel plates.

## C. Scanning Procedure

Koristka 30X objectives of 3000 $\mu$ working distance were used with 20X and 30X oculars. This permitted the observation of minimum-ionizing tracks through the mounting glass in both pellicles. The projected angle of each minimum-ionizing track crossing a line perpendicular to the beam was recorded. Tracks at angles greater than 4.5° to the average beam direction were tested to see if they could be traced through the interface. A track that terminated at the interface was presumably not part of the beam. Each track was examined over a length sufficient to distinguish knock-on electrons.

Area scanning for pion stars in emulsion stacks placed

in front of and behind the iron "foil" provided an estimate of the pion contamination independent of that of Masek et al.[6] and Kim et al.[7]

## IV. MEASUREMENTS

### A. Structure of the Incident Beam

The density of minimum tracks incident on the forward stack was $2.9\times10^4$ cm$^{-2}$ at the median plane of the beam and $1.5\times10^4$ cm$^{-2}$ 10 in. from the median plane. The projected angular distribution at the median plane is shown in Fig. 3(a). Tracks in the extremes of this distribution must be those of particles which suffered scatterings in the targets and scintillators of the counting experiment, which were traversed prior to reaching the first emulsion detector.

### B. The Pion Contamination

In the forward stack 22 stars with a minimum-ionizing prong parallel to the beam and at least one heavy prong were found in an area $31.5\times6$ cm$^2$ in a 600$\mu$ pellicle. Assuming all of these to be interactions of beam pions, and using 40 cm as the pion mean free path for interactions of this type gives 880 cm of pion track in the volume, or a pion density of $\approx10^2$ cm$^{-2}$ in the beam. Over the same region the average density of minimum-ionizing tracks is $2.5\times10^4$ cm$^{-2}$, leading to a pion contamination of approximately $\frac{1}{2}\%$ at this point. Kim et al. deduce a pion contamination of $(1.3\pm0.2)\%$[7] at this position for tracks within $\pm1°$ of the central beam direction, and Masek et al. measured the pion contamination of the beam incident on the targets to be 3%.[6] In the area scan in the stack behind the scatterer, only 12 stars with minimum-ionizing prongs were found in 3 cm$^3$ of emulsion. Since the angular distribution of these minimum tracks was consistent with isotropy, no measurement of the pion contamination could be made at this position. We take 2% as an approximate upper limit on the pion contamination ahead of the scatterer. Since approximately 90% of the pions are absorbed in the 18 in. of iron, the contamination behind the iron is less than about 0.2%. Therefore, it is not a significant contributor to the moments.

### C. The Emergent Beam

The angular distribution of 3475 tracks after traversal of the scatterer is shown in Fig. 3(b). Small corrections have been made for the tracks that could not be tested by tracing them through the interface. Some went out the edge of the pellicle or for other reasons could not be tested.

## V. CALCULATIONS

### A. Calculation of the Moments of the Observed Distributions

The moments of the observed distributions are given by $\phi^{2m}=(1/\sum n_i)\sum n_i\Delta_i^{2m}$, where $\Delta_i$ is the deviation of

| | Incident | Emergent |
|---|---|---|
| $\langle\phi^2\rangle$ | 0.783 | 8.52 |
| $\langle\phi^4\rangle$ | 2.75 | 231 |
| $\langle\phi^6\rangle$ | 22.5 | $1.18\times10^4$ |
| $\langle\phi^8\rangle$ | 272 | $9.16\times10^5$ |
| $\langle\phi^{10}\rangle$ | 3970 | $9.08\times10^7$ |
| $\langle\phi^{12}\rangle$ | $6.45\times10^4$ | $1.03\times10^{10}$ |
| $\langle\phi^{14}\rangle$ | $\cdots$ | $1.27\times10^{12}$ |
| $\langle\phi^{16}\rangle$ | $\cdots$ | $1.63\times10^{14}$ |

the $i$th interval from the mean and $n_i$ is the number of events in this interval. The moments of the observed distributions needed to calculate primary distribution moments up to the eighth and their errors are shown in Table I. Sheppard's correction[12] has been applied to the second and fourth moments. The moments of the multiple-scattering distribution in the iron can be related to the moments of the observed distributions ahead of and behind the scatterer by a derivation analogous to that given in Sec. II. This derivation gives the following relations, where $\phi$ refers to the distribution in the scatterer and $\phi_1$ and $\phi_2$ refer to the observed distributions before and after traversal of the scatterer:

$$\langle\phi^2\rangle=\langle\phi_2^2\rangle-\langle\phi_1^2\rangle,$$

$$\langle\phi^4\rangle=\langle\phi_2^4\rangle-\langle\phi_1^4\rangle-6\langle\phi^2\rangle\langle\phi_1^2\rangle,$$

$$\langle\phi^6\rangle=\langle\phi_2^6\rangle-\langle\phi_1^6\rangle-15(\langle\phi_1^2\rangle\langle\phi^4\rangle+15\langle\phi_1^4\rangle\langle\phi^2\rangle),$$

$$\langle\phi^8\rangle=\langle\phi_2^8\rangle-\langle\phi_1^8\rangle-70\langle\phi_1^4\rangle\langle\phi^4\rangle$$
$$-28(\langle\phi_1^6\rangle\langle\phi^2\rangle+\langle\phi_1^2\rangle\langle\phi^6\rangle),\quad \text{etc.}$$

These expressions, combined with the equations of Sec. II, give the following equations for the moments of the primary scattering distribution in iron:

$$n\langle\omega^2\rangle=\langle\phi_2^2\rangle-\langle\phi_1^2\rangle,$$

$$n\langle\omega^4\rangle=\langle\phi_2^4\rangle-3\langle\phi_2^2\rangle^2-\langle\phi_1^4\rangle+3\langle\phi_1^2\rangle^2,$$

$$n\langle\omega^6\rangle=\langle\phi_2^6\rangle-15\langle\phi_2^4\rangle\langle\phi_2^2\rangle+30\langle\phi_2^2\rangle^3$$
$$-\langle\phi_1^6\rangle+15\langle\phi_1^4\rangle\langle\phi_1^2\rangle-30\langle\phi_1^2\rangle^3,$$

and
$$(10)$$

$$n\langle\omega^8\rangle=\langle\phi_2^8\rangle-28\langle\phi_2^6\rangle\langle\phi_2^2\rangle-35\langle\phi_2^4\rangle^2$$
$$+420\langle\phi_2^4\rangle\langle\phi_2^2\rangle^2-630\langle\phi_2^2\rangle^4-\langle\phi_1^8\rangle$$
$$+28\langle\phi_1^6\rangle\langle\phi_1^2\rangle+35\langle\phi_1^4\rangle^2$$
$$-420\langle\phi_1^4\rangle\langle\phi_1^2\rangle+630\langle\phi_1^2\rangle^4.$$

The variances of these quantities are given by

$$\sigma^2(n\langle\omega^{2m}\rangle)=\sum\left(\frac{\partial(n\langle\omega^{2m}\rangle)}{\partial N_{1i}}\right)^2 N_{1i}+\sum\left(\frac{\partial(n\langle\omega^{2m}\rangle)}{\partial N_{2i}}\right)^2 N_{2i}.$$

The values of the $n\langle\omega^{2m}\rangle$ are:

$$n\langle\omega^2\rangle=(2.33\pm0.06)\times10^{-3}\text{ rad}^2,$$

$$n\langle\omega^4\rangle=(1.42\pm0.81)\times10^{-6}\text{ rad}^4,$$

$$n\langle\omega^6\rangle=(3.04\pm1.17)\times10^{-8}\text{ rad}^6,\qquad(11)$$

and

$$n\langle\omega^8\rangle=(-7.4\pm27.8)\times10^{-10}\text{ rad}^8.$$

## B. Moments of the Single Scattering Laws

The projected-angle single scattering law for a point nucleus as given by Molière[4] may be written

$$f(\omega)=\tfrac{1}{2}Q[1/(\omega^2+\omega_m^2)^{3/2}],\qquad(12)$$

where $\omega_m$ is the atomic-screening constant.

To allow for a finite nucleus, Rainwater and Cooper[14] modify this to

$$f(\omega)=\tfrac{1}{2}Q[F_N(\omega/\omega_0)/(\omega^2+\omega_m^2)^{3/2}],\qquad(13)$$

where $F(\omega/\omega_0)$ is the nuclear form factor and $\omega_0=\lambda/R$. The quantity $2\pi\lambda$ is the wavelength of the scattered particle and $R$ is the radius of the target nucleus. Energy loss in the iron was allowed for by using the average effective momentum of the muons in the expressions for $\omega_m$ and $\omega_0$. It is 1700 MeV/$c$.

For the nuclear form factor, Rainwater and Cooper give

$$F_N(\omega/\omega_0)=F_N{}^c+(1/Z)(1-F_N{}^c),$$
$$F_N{}^c=1, 0.82, 0.50, \text{ and } 0.15$$
$$\text{for } (\omega/\omega_0)=0, 1, 2, 3,\qquad(14)$$

and

$$F_N{}^c=12/(\omega/\omega_0)^4 \text{ for } (\omega/\omega_0)\geqslant4.$$

We approximated this with the expression

$$F_N{}^c=1-0.0733(\omega/\omega_0)-0.125(\omega/\omega_0)^2$$
$$+0.0183(\omega/\omega_0)^3 \text{ for } (\omega/\omega_0)\leqslant3,$$

and

$$F_N{}^c=12(\omega/\omega_0)^4 \text{ for } (\omega/\omega_0)>3.$$

The moments are then given by

$$\langle\omega^{2m}\rangle=\int_0^B \omega^{2m}f(\omega)d\omega\Big/\int_0^B f(\omega)d\omega.\qquad(15)$$

The upper limit of these integrations, $B$, reflects the biases of our observations. The intensity of the incident beam decreases slowly to one-half maximum at 25 cm from the centerline, and our measurements on the emergent beam were made within 5 cm of the centerline. Therefore, since the projected rms displacement of the beam is only approximately 1.3 cm after traversal of

TABLE II. Comparison of elementary scattering moments.

| | Experimental | Rainwater, Cooper | Molière |
|---|---|---|---|
| $\langle\omega^2\rangle$ (rad$^2$) | $(5.70\pm0.15)\times10^{-10}$ | $5.88\times10^{-10}$ | $7.74\times10^{-10}$ |
| $\langle\omega^4\rangle$ (rad$^4$) | $(3.5\pm2.0)\times10^{-13}$ | $2.37\times10^{-13}$ | $24.1\times10^{-13}$ |
| $\langle\omega^6\rangle$ (rad$^6$) | $(7.4\pm2.9)\times10^{-15}$ | $4.01\times10^{-15}$ | $82.7\times10^{-15}$ |
| $\langle\omega^8\rangle$ (rad$^8$) | $(-1.8\pm6.8)\times10^{-16}$ | $1.6\times10^{-16}$ | $38\times10^{-16}$ |
| $\langle\omega^4\rangle/\langle\omega^2\rangle$ (rad$^2$) | $(6.2\pm5.8)\times10^{-4}$ | $4.03\times10^{-4}$ | $31.1\times10^{-4}$ |
| $\langle\omega^6\rangle/\langle\omega^2\rangle$ (rad$^4$) | $(1.2\pm0.5)\times10^{-5}$ | $0.682\times10^{-5}$ | $10.7\times10^{-5}$ |

[14] L. N. Cooper and J. Rainwater, Phys. Rev. 97, 492 (1955).

the scatterer, we have no appreciable geometrical bias. We used for $B$ the largest angle actually observed, 15 deg. We have not considered the proton form factor in calculating these moments. In Table II, we compare these moments with the elementary-scattering distribution moments calculated from the data, using expression (7) to calculate the effective number of collisions. It gives $n = 4.09 \times 10^6$. Also, in Table II the ratios

$$\frac{\langle\omega^4\rangle}{\langle\omega^2\rangle} = \frac{\langle\phi_2{}^4\rangle - \langle\phi_1{}^4\rangle - 3\langle\phi_2{}^2\rangle^2 + 3\langle\phi_1{}^2\rangle^2}{\langle\phi_2{}^2\rangle - \langle\phi_1{}^2\rangle} \tag{16}$$

and

$$\frac{\langle\omega^6\rangle}{\langle\omega^2\rangle} = \frac{\langle\phi_2{}^6\rangle - 15\langle\phi_2{}^4\rangle\langle\phi_2{}^2\rangle + 30\langle\phi_2{}^2\rangle^3 - \langle\phi_1{}^6\rangle + 15\langle\phi_1{}^4\rangle\langle\phi_1{}^2\rangle - 30\langle\phi_1{}^2\rangle^3}{\langle\phi_2{}^2\rangle - \langle\phi_1{}^2\rangle}$$

are compared with those calculated for the two elementary distributions. These quantities are independent of the effective number of collisions.

Although some of the experimental uncertainties are comparable to the magnitude of the measured quantity, these errors are all much less than the moments predicted for a point-nucleus model. The experiment also serves very well to illustrate how the theory of moment propagation may be applied practically.

## ACKNOWLEDGMENTS

# Elastic $K^+$-Proton Scattering at 970, 1170, and 1970 MeV/c*

V. Cook, D. Keefe, L. T. Kerth, P. G. Murphy,† W. A. Wenzel, and T. F. Zipf

*Lawrence Radiation Laboratory, University of California, Berkeley, California*

(Received 29 October 1962)

A liquid-hydrogen target surrounded by spark chambers was used to study $K^+$-proton elastic scattering at 970, 1170, and 1970 MeV/c incident $K^+$ momentum. In contrast with results at lower energies, the angular distributions were not isotropic; the anisotropy increases with energy, while the elastic cross section decreases. A number of phase-shift solutions using (a) $S_{1/2}$, $P_{1/2}$, and $P_{3/2}$ complex phase shifts; (b) real $S_{1/2}$, $P_{1/2}$, and $P_{3/2}$, and complex $D_{3/2}$ phase shifts; and (c) complex $S_{1/2}$ and $D_{3/2}$, and real $P_{1/2}$ and $P_{3/2}$ phase shifts have been found for the 970- and 1170-MeV/c data. The 1970-MeV/c distribution has been fitted by an optical model. The data presented here have been included with other information on $K$-nucleon scattering in a test of forward-scattering dispersion relations. The data are still insufficient to provide a definitive test; however, an acceptable fit was found for $\Gamma$ (effective pole residue) $= -0.1 \pm 0.3$.

## 1. INTRODUCTION

PREVIOUS experiments on the interaction of $K^+$ mesons with nucleons include investigations at low energies of the total and elastic cross sections by means of emulsions (0 to 600 MeV/c),[1] counters (500 to 600 MeV/c),[2] the propane bubble chamber,[3] and the 15-in. Berkeley liquid-hydrogen bubble chamber (100 to 810 MeV/c).[4]

In the region above 810 MeV/c, the only data hitherto available have been total $K^+$-$p$ and $K^+$-$n$ cross-section measurements from counter experiments by Burrowes et al. (up to 2.5 BeV/c)[5]; von Dardel et al. (2.9 to 6 BeV/c)[6]; Vovenko et al. (2 to 4 BeV/c)[7]; Cook et al.

* Work done under the auspices of the U. S. Atomic Energy Commission.

† On leave from Rutherford High Energy Laboratory, Harwell, England.

[1] D. Keefe, A. Kernan, A. Montwill, M. Grilli, L. Guerriero, and G. A. Salandin, Nuovo Cimento 12, 241 (1959).

[2] T. F. Kycia, L. T. Kerth, and R. G. Baender, Phys. Rev. 118, 553 (1960).

[3] D. I. Meyer, D. A. Glaser, and M. L. Perl, Phys. Rev. 107, 279 (1957).

[4] T. F. Stubbs, H. Bradner, W. Chinowsky, G. Goldhaber, S. Goldhaber, W. Slater, D. M. Stork, and H. K. Ticho, Phys. Rev. Letters 7, 188 (1961).

[5] H. C. Burrowes, D. O. Caldwell, D. H. Frisch, D. A. Hill, D. M. Ritson, and R. A. Schluter, Phys. Rev. Letters 2, 117 (1959).

[6] G. von Dardel, D. H. Frisch, D. Mermod, R. H. Milburn, P. A. Piroué, M. Vivargent, G. Weber, and K. Winter, Phys. Rev. Letters 5, 333 (1960).

[7] A. S. Vovenko, B. A. Kulakov, M. F. Lykhachev, A. L.